Peptide-Assisted Design of Precision Polymer Sequences: On the Relevance of the Side-Chain Sequences and the Variability of the Backbone

*Sensu Celasun, Eva Maron, and Hans G. Börner**

Functional sequences of monodisperse, sequence-defined oligo(amide-urethane)s are designed based on a peptide sequence as blueprint. The translation of a discrete side-chain functionality sequence from a known peptide-based solubilizer of the photosensitizer *meta*-tetra(hydroxyphenyl)-chlorin, into a non-peptidic precision polymer backbone is demonstrated. The resulting peptidomimetic precision polymers retain the functions of the parent peptide sequence, showing analogues sensitivity toward single monomer mutations/exchanges and even exceeding the parent peptide equivalent by reaching up to 69% higher payload capacities and more favored release kinetics.

Rebuilding functional minimal sequences of proteins with non-α-amino acid building blocks proved to be one of the potent strategies to access functional peptidomimetics.[1,2] The approach was utilized for the realization of synthetic analogues based on biologically active peptides like antimicrobial peptides,[3,4] cell penetrating peptides,[5,6] peptide-based hormones,[7] or HIV-Tat nuclear localization signals.[8,9] Particularly oligopeptides offer a suitable platform as sequence–structure–function relationships are often well understood or can be predicted by computational simulation. Moreover, (bio) combinatorial approaches such as split and mix libraries, phage display biopanning or peptide array technologies, as well as mass spectrometry sequencing and interaction profiling are routinely available for the peptides, holding the promise to reveal functional sequences.[10–14] Those established tools enabled the exploitation of peptides in materials sciences, where peptide applications span from programmable nanostructure formation for biomedicine or nanoelectronics, to the direction of hierarchically ordered hybrid materials, to bioactive material interfaces, surface specific coatings, material specific compatibilizers as well as drug structure specific solubilizers or enzymatically activable glues.[15–24] Recently, the direct translation of a peptide sequence toward peptide-structure related precision polymers was demonstrated.[25] The peptide was identified by combinatorial means for drug hosting and solubilization of *meta*-tetra(hydroxyphenyl)-chlorin (*m*-THPC) as one of the promising second generation photosensitizers for the photodynamic cancer therapy.[26] The peptide sequence was effectively mimicked by monodisperse precision segments based on either heptamer oligo(2-substituted α-hydroxyl acid)s or pentamer oligo(*N*-substituted acrylamide)s.[25] Those precision segments exhibited discrete side-chain sequences, which match the peptide side-chains in functionality and order. The approach proved to be valid, as the corresponding poly(ethylene glycol) (PEG) conjugates of those precision segments mimicked the drug solubilizer properties of the parent peptide-PEG conjugate, by reaching up to 40% higher payloads and showing more desired drug release profiles. These precision polymer platforms were ideal for the exploration of peptidomimetic precision segments, as peptides show chemical similarities with oligo(*N*-substituted acrylamide)s and structural similarities to oligo(2-substituted-α-hydroxy acid)s. Within the last decade, sequence-defined polymers have been set into the focus of polymer chemistry,[27–31] because this class of macromolecules enables envisioning the realization of highly selective functions as found within information-rich biomacromolecules like RNA/DNA, oligosaccharides and peptides/proteins.[32,33] Meanwhile, elegant and efficient means have been established to synthesize precision polymers, exploiting both solid-phase supported and solution synthesis routes based on a variety of backbone chemistries and rapidly growing sets of fully synthetic monomer libraries.[34–38] While some precision polymers are closely related to existing classes of biomacromolecules like for instance peptoids or nucleotide resembling polymers,[34,39] several precision platforms explore more widely the chemical space available for backbone and side chain chemistries.[40–42] Among the latter, thiolactone-based oligo(amide-urethane)s have shown to be a versatile precision polymer platform.[43] Du Prez et al. introduced the type of polymer and described a route by solid phase supported submonomer synthesis.[44] The two step synthesis protocol relies on thiolactone (Tla)/Michael chemistry and made a large set of monomers available by reacting different acrylates in the second synthesis step of the reaction cycle.[42] Previously, a combinatorial strategy was demonstrated to screen an one-bead one-compound (OBOC) library

S. Celasun, E. Maron, Prof. H. G. Börner
Laboratory for Organic Synthesis of Functional Systems
Department of Chemistry
Humboldt-Universität zu Berlin
Brook-Taylor-Str. 2, 12489 Berlin, Germany
E-mail: h.boerner@hu-berlin.de

The ORCID identification number(s) for the author(s) of this article can be found under https://doi.org/10.1002/mabi.201900244.

DOI: 10.1002/mabi.201900244

of oligo(amide-urethane) precision polymers against *m*-THPC to identify sequence domains with high binding capacities.[45] Corresponding PEG-conjugates result in precision formulation additives, where the sequence proved to sensitively influence the *m*-THPC hosting and release properties.

While the combinatorial OBOC route proved to reveal functional precision segments, the direct translation of oligopeptides to precision polymer backbones by monomer-to-monomer mapping of the peptide side-chain functionalities appears to be more straightforward and demands less synthetic efforts.

Herein, we investigate the scope to broaden the strategy of direct sequence translation from a functional peptide into a sequence of a precision polymer that is chemically and structurally unrelated to a peptide. The *m*-THPC hosting peptide domain was taken as template and a monodisperse precision polymer from the type of thiolactone-based oligo(urethane-amide)s was synthesized as a PEG-conjugate. The drug hosting and release properties of a set of PEG-precision conjugates, which exhibited single side sequence mutations, has been analyzed and the relevant properties were compared to those of the parent peptide-PEG conjugate.

The previously analyzed peptide-PEG conjugate QFFLFFQ-PEG solubilized *m*-THPC and reached payload capacities of up to 1:3.3 (molar ratio drug:carrier).[26] The systematic alanine substitution (Ala-scan) revealed the hydrophobic core domain FFLFF as the segment of importance for drug hosting.[25,46] While an exchange of the polar Gln1 or Gln7 residues increased the capacity by up to 39%, the substitution of the central residue Leu4 by Val or Ala residues reduced the payload dramatically by up to 92%.[25] Moreover, the polar peptidic backbone and the amide side chain functionalities of the flanking Gln residues were required to accelerate the drug release.[25,46] A removal or substitution of both polar Gln1 and Gln7 residues lead to undesired slow release kinetics, whereas the exchange of only one Gln residue preserved the fast release profile. Taking those sequence related properties of the peptide-PEG conjugate into account, a set of oligo(amide-urethane) precision polymers was designed (**Figure 1**). The target sequence originated from monomer-to-monomer mapping, by translating the relevant peptide side-chain functionality-sequence of a minimal binding motif into the precision polymer backbone (Figure 1). The flanking Gln-analogue residues have been not included into the sequence design, as it was hypothesized that the extended polar backbone structure of the oligo(amide-urethane) precision segment provides sufficient polarity to counterbalance their removal.

The precision polymer set was synthesized by the iterative thiolactone (Tla)/Michael submonomer synthesis on a PEG

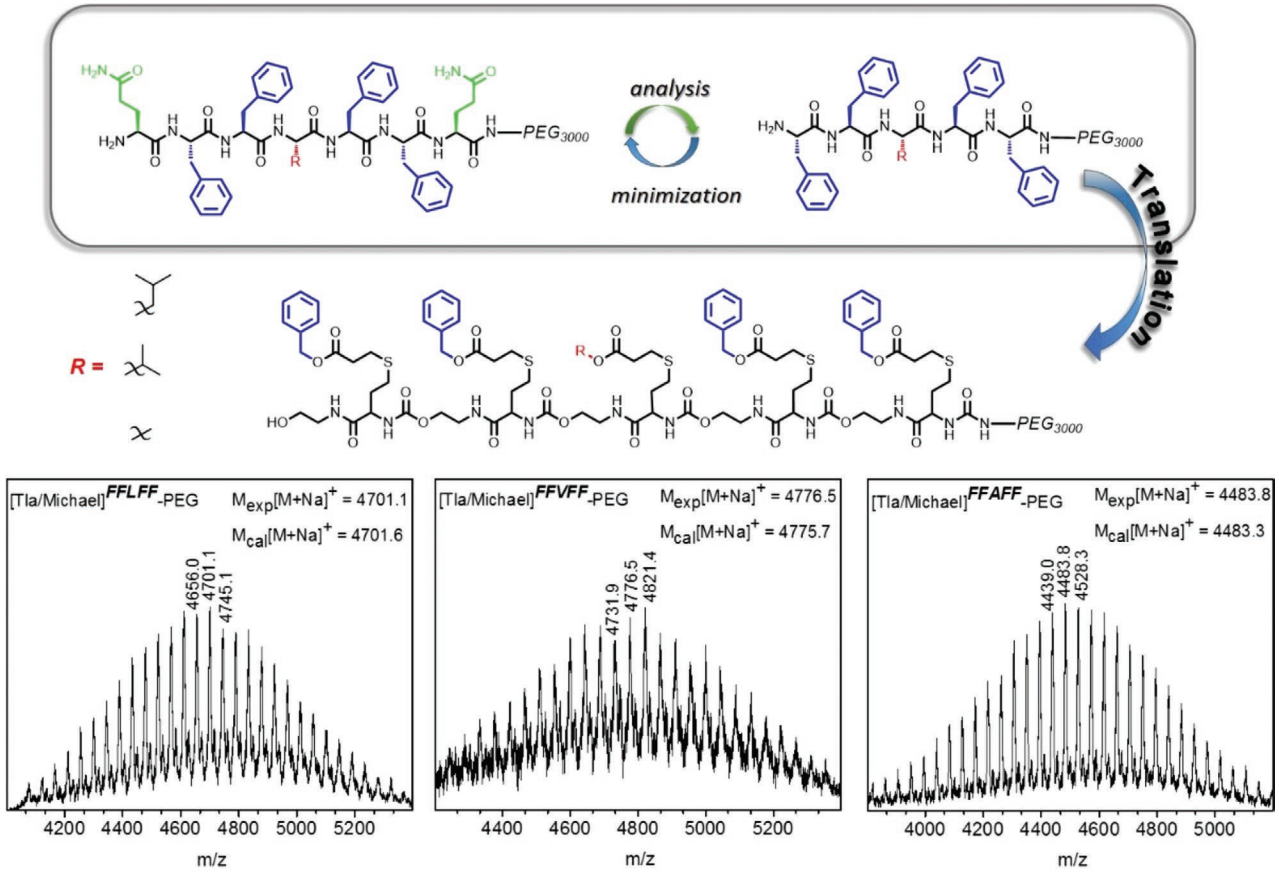

Figure 1. Representation of the sequence transfer strategy, translating a functional peptide-PEG conjugate after sequence minimization into a corresponding PEG-conjugated precision sequence (top/middle) and MALDI-TOF MS analysis data of the PEG-*block*-oligo(amide-urethane) precision polymers ***[Tla/Michael]^{FFLFF}-PEG***, ***[Tla/Michael]^{FFVFF}-PEG***, and ***[Tla/Michael]^{FFAFF}-PEG*** (bottom, from left to right; for detailed assignments, see Supporting Information).

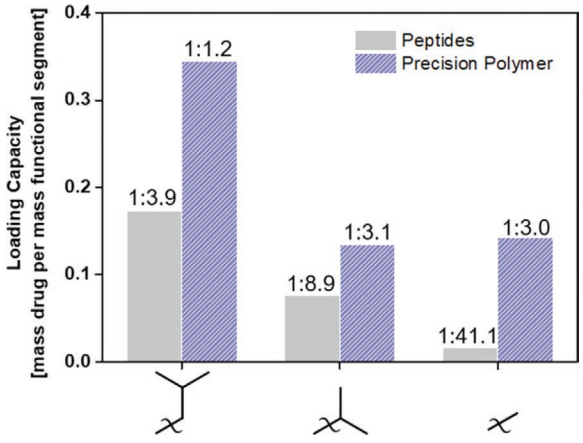

Figure 2. Drug loading capacities of PEG-conjugates with precision polymer or peptide segments are specified as normalized values to the masses of the functional segments (corresponding molar ratio drug:carrier are provided on top of each column).

preloaded poly(styrene) resin (PAP resin) to directly obtain (Tla/Michael)-PEG conjugates with PEG blocks of M_n = 3000 Da and $Đ$ = 1.04.[47] Due to the polarity of the support an adapted synthesis protocol had to be applied, where isocyanate thiol-actone coupling and aminolysis steps have been enforced.[48] The platform of oligo(amide-urethane) precision polymers, allows to define the side chain functionalities by employing different acrylic acid esters in the presence of 2-aminoethanol for the aminolysis/Michael thiol-ene reaction step. Thus, benzyl acrylate, isobutyl acrylate, isopropyl acrylate, and methyl acrylate build up the analogue monomer alphabet to mimic Phe, Leu, Val, and Ala, respectively (Figure 1). A [Tla/Michael]-PEG conjugate, with a side chain sequence based on the core segment of the parent peptide FFLFF was synthesized (***[Tla/Michael]^{FFLFF}-PEG***). Moreover, the two single point mutations in the central position realized in ***[Tla/Michael]^{FFVFF}-PEG*** and ***[Tla/Michael]^{FFAFF}-PEG*** a systematic reduction of the hydrophobicity by exchanging the Leu3-analogue residue to Val- or Ala-analogues (**Figure 2**, Supporting Information).

The set of PEGylated precision polymers was cleaved from the support and ^{1}H-NMR, IR as well as MALDI-TOF MS analyses verified the structural and chemical identity of the compounds (cf. Figure 1; Supporting Information). All samples were readily soluble in aqueous media. M-THPC loading experiments were performed by following enforced drug loading procedures.[26] Interestingly, all three conjugates ***[Tla/Michael]^{FFLFF}-PEG***, ***[Tla/Michael]^{FFVFF}-PEG***, and ***[Tla/Michael]^{FFAFF}-PEG*** were able to reach higher payload capacities for *m*-THPC in comparison to their peptide-PEG analogues (Figure 2). The precision polymer PEG-conjugate ***[Tla/Michael]^{FFLFF}-PEG*** that originated from the direct translation of the parent peptide, reached a payload of 1:1.2 (molar ratio drug:carrier), which is about 69% higher compared to the value found by the peptide-PEG conjugate under similar conditions. For comparability reasons, the capacity values shown in Figure 2, were normalized to the mass fraction of the functional segment (peptide or oligo(amide-urethane)). The side chain spacing along the backbone of the precision segment is expected to be larger and the conformational freedom of the side chain and backbone is significantly higher compared to amino acids in the parent 7*mer* oligopeptide. This might enable the formation of a more optimized interface between the precision segment and the drug. The flexibility might reduce the formation of "frustrated" segments that cannot participate in drug binding, which would explain the higher drug binding capacity of the precision segment compared to the peptide.

Comparing the drug loading capacities of the set of precision conjugates, which have single point mutations, revealed an obvious decrease between ***[Tla/Michael]^{FFLFF}-PEG*** and both ***[Tla/Michael]^{FFVFF}-PEG*** and ***[Tla/Michael]^{FFAFF}-PEG*** by reaching payload capacities of 1:1.2, 1:3.1, and 1:3.0, respectively (molar ratio drug:carrier) (Figure 2). Interestingly, peptide-PEG conjugates show also a high sensitivity of the *m*-THPC loading capacity on central Leu4 residue exchange by Val and Ala. In both, the [Tla/Michael]-PEG and the peptide-PEG conjugates the payload reduces similarly by about 60%, if ***QFFLFFQ-PEG*** or ***[Tla/Michael]^{FFLFF}-PEG*** were compared to ***QFFVFFQ-PEG*** or ***[Tla/Michael]^{FFVFF}-PEG***, respectively. The significantly affected payload capacity in the precision-PEG system by the exchange of a single isobutyl to isopropyl side chain functionality remains remarkable. It should be noted, that the [Tla/Michael] segment compared to the peptide exhibits both a higher conformational flexibility and a higher weight fraction of the backbone structure versus the variable side chain functionalities. Where the parent peptide QFFLFFQ shows 42 wt% contributed by the backbone and 58 wt% by the side chains, the precision analogue ***[Tla/Michael]^{FFLFF}*** exhibits 77 wt% of a constant backbone structure and only 23 wt% result from the variable side chains. Hence, a change of side chain functionality is expected to have less impact on the precision system properties because only a minor fraction is changed. Moreover, the side chain functionality in the precision segment is not tightly coupled to the backbone structure due to an extended and flexible spacer. However, the reduction by $-CH_2-$ in only one side chain, lowers the payload capacity by 62%. Such an obvious effect is certainly surprising, but indicates sharply defined sequence–property relationships as predicted for monodisperse oligomers. The reduction in payload is even more pronounced in the peptide system, lowering the capacity of ***QFFVFFQ-PEG*** to ***QFFAFFQ-PEG*** further by 58% to reach only 8%, of the capacity from the parent ***QFFLFFQ-PEG*** conjugate. In contrast to this, a reduction cannot be found in the respective precision conjugates (***[Tla/Michael]^{FFVFF}-PEG*** versus ***[Tla/Michael]^{FFAFF}-PEG***), as the Val to Ala analogues reached rather similar capacities (Figure 2). This suggests that the found effect is not simply due to a decrease in volume fraction of the hydrophobic segment and makes specific binding interactions between [Tla/Michael] domains and *m*-THPC likely.

Dynamic light scattering (DLS) measurements of the set of precision polymer conjugates were performed prior and after *m*-THPC loading to provide insights into the type of solubilization (**Figure 3**). Monomodal size distributions of the drug loaded complexes with hydrodynamic radii (R_h) in the range of 42–55 nm and low polydispersity indices < 0.1 indicate the presence of well-defined colloidally stable aggregates in aqueous solution. The aggregate sizes are in a range to exclude discrete micelle formation and suggest the presence of more

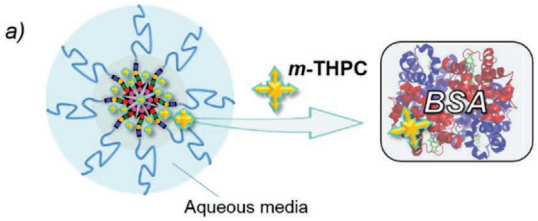

b)

Solubilizer	- *m*-THPC	+ *m*-THPC	
	R_h (nm)	R_h (nm)	PDI
[Tla/Michael]^{FFLFF}-PEG	n.a.	42	0.064
[Tla/Michael]^{FFVFF}-PEG	n.a.	50	0.059
[Tla/Michael]^{FFAFF}-PEG	n.a.	55	0.002

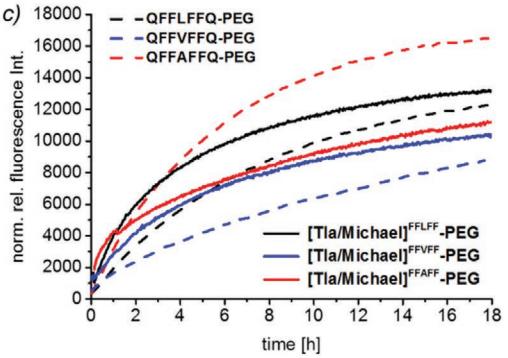

Figure 3. Photosensitizer solubilization and release kinetics of *m*-THPC from oligo(amide-urethane)-PEG conjugate complexes. a) Schematic illustration of the trans-solubilization of *m*-THPC from colloidal drug/solubilizer complexes to albumins as blood plasma protein models, b) DLS analysis of the set of precision polymer conjugates prior and after *m*-THPC loading, and c) drug release kinetics from *m*-THPC/solubilizer complexes to bovine serum albumin (conditions: λ_{ex} = 417 nm, λ_{em} = 653 nm, c[BSA] = 100 µM, c[*m*-THPC] = 0.1 µM; n.a. = not analyzable due to multimodal size distributions).

complex non-equilibrium structures. This was supported by cryo-transmission electron microscopy (cryo-TEM) analysis of a representative drug/solubilizer complex (cf. Figure S4, Supporting Information). The cryo-TEM images of an aqueous solution of *m*-THPC/***[Tla/Michael]^{FFAFF}-PEG*** exhibit isotropic aggregates with rather homogeneous contrast distribution and reveal an average radius of about 50 nm, which agrees very well with the findings from DLS proving a R_h of 55 nm. Obviously, the DLS analysis results indicate that differences in loading capacity of the three [Tla/Michael]-PEG conjugates were not resulting from a dramatic change of the aggregate sizes. As the sizes of the drug/solubilizer complexes remain well below 100 nm with relatively low polydispersity indices they appear suitable for biomedical applications, for example, for the photodynamic cancer therapy.[49] In the absence of the drug, all precision polymer conjugates exhibit in dilute solutions multimodal size distributions (data not shown), which suggest the presence of dynamic, ill-defined aggregates. This could be expected for oligo(amide-urethane)-*block*-PEG copolymers, having the possibility for various intermolecular interactions between the functional segments.

It seems to be noteworthy, that ***[Tla/Michael]^{FFLFF}-PEG*** shows even a higher drug payload capacity compared to the best performing candidate resulting from a recently described combinatorial screening of a library of sequences based on the same type of oligo(amide-urethane) precision polymers.[45] This can be rationalized by the presence of two benzyl dyads in ***[Tla/Michael]^{FFLFF}-PEG***, whereas the sequences found by the combinatorial approach exhibit only one benzyl dyad. From the peptide sequence analysis the importance of benzyl dyads to contribute to the payload capacity was indicated.[46] It should be emphasized, that the combinatorial screening was successfully identifying unknown high capacity binding sequences. However, as common in combinatorial approaches, several sequence candidates need to be tested to reveal the best performers from the pool of screening results. In one-bead one-compound library-screening assays, also secondary selection criteria like sequence solubility, segment self-aggregation or segment interactions with the support are relevant to modulate the availability of the supported sequences and influence the screening results.

Drug loading capacity constitutes only one of the important parameters for drug solubilization and transport. Particularly, the class of precision formulation additives offers the capability to fine-tune drug release kinetics, by controlling the drug-solubilizer interactions precisely. This parameter could be included actively in the selection procedure.[50] As recently demonstrated in a 2D screening, peptide sequences can be selected for both high capacity drug binders and tailored drug release profiles. However, the QFFLFFQ originated from an earlier study and drug release kinetics could be analyzed by a fluorescence spectroscopy assay.[26] This enabled to follow the trans-solubilization of *m*-THPC from drug/solubilizer complexes toward albumin (bovine serum albumin, BSA) as a blood plasma protein model. During the transfer of the drug from solubilizer complexes to BSA, the fluorescence activity and singlet oxygen production capability of *m*-THPC were regained.[26] In many drug delivery applications, a strong drug binding is required for effective drug transport.[51,52] Nonetheless, the concept of drug solubilizers profits from a transient binding and a rapid drug release to blood plasma proteins.[26] Those inbuilt biotransport systems, will be responsible for systemic distribution in a potential therapeutic application.[53,54] A fast release of *m*-THPC is beneficial for a rapid activation of the photosensitizer to prevent adverse effects like extended light sensitivity of patients.[55]

Similarly, to the *m*-THPC/peptide-PEG complexes, the fluorescence activity of *m*-THPC/[Tla/Michael]-PEG complexes was fully quenched, but fluorescence was regained after the addition of BSA. Hence, similar mechanisms can be anticipated, suggesting that BSA triggers the transsolubilization of the drug to form fluorescence active *m*-THPC/BSA complexes. The release profiles of *m*-THPC from drug-loaded [Tla/Michael]-PEG solubilizers showed a related type as compared to these, found in *m*-THPC/peptide-PEG complexes (Figure 3). The release kinetics of the parent *m*-THPC/***QFFLFFQ-PEG*** complex were quite similar to those of the *m*-THPC/***[Tla/Michael]^{FFVFF}-PEG*** and *m*-THPC/***[Tla/Michael]^{FFAFF}-PEG*** complexes. The drug release from the *m*-THPC/***[Tla/Michael]^{FFLFF}-PEG*** complex, where the directly copied precision sequence was utilized, appears to be faster and even more effective. While under these conditions ≈60% of the releasable drug was released from the *m*-THPC/***[Tla/Michael]^{FFLFF}-PEG*** complexes within 3 h, only ≈40% of the releasable drug was activated from *m*-THPC/***QFFLFFQ-PEG*** complex with the parent peptide solubilizers. Also, the half-release time ($t_{1/2}$), where 50% of the releasable drug is activated, was more favorable in the precision system. While the *m*-THPC/***[Tla/Michael]^{FFLFF}-PEG*** complexes reached $t_{1/2}$ of 2 h, the *m*-THPC/***QFFLFFQ-PEG*** complexes had under comparable conditions a $t_{1/2}$ of 4.5 h. Interestingly, both solubilizer systems, peptide-PEG and [Tla/Michael]-PEG indicated similar sensitivity of the initial *m*-THPC release rates on the central residue exchange (Figure 3; Table S1, Supporting Information). The sequence variants with Ala or Ala-analogue residues exhibit the highest initial release rates of *m*-THPC from the respective drug/solubilizer complexes. This was followed by sequences with Leu/Leu-analogue residues, having lower and sequences with Val/Val-analogue residues exhibiting the lowest initial release rates. The correlation between the respective sequence variants of both peptide and oligo(amide-urethane) segments is certainly notable. This analogy seems to be a remarkable finding, as the oligomer platforms, which were compared in this study exhibit rather dissimilar backbone chemistries, structures, and conformational dynamics. Nonetheless, the similar sensitivities of properties on sequence variations proved that the translation of side-chain functionality sequences across unrelated backbone platforms is feasible. Property trends can be transferred to the peptidomimetic polymers, even if, several factors at the molecular level are influencing the drug loading and release profiles within the kinetically controlled loading procedure and the interface controlled trans-solubilization process.

In conclusion, the side chain functionality sequence of the functional peptide QFFLFFQ was translated into a precision polymer segment, based on monodisperse oligo(amide-urethane)s ([Tla/Michael] precision polymer). The peptide has been selected recently by combinatorial means and the corresponding peptide-PEG conjugate proved to be a capable solubilizer for the photosensitizer *m*-THPC. The PEGylated precision segment ***[Tla/Michael]^{FFLFF}-PEG*** not only retained properties of the parent ***QFFLFFQ-PEG*** conjugate, but reached 69% higher payload capacities as well as more desired drug release properties. Sets of peptide-PEG and [Tla/Michael]-PEG solubilizers were accessed by systematic sequence variations, substituting the central Leu/Leu-analogue residue by Val and Ala or their respective analogue residues. The study confirmed the presence of sharply defined sequence–property relationships in monodisperse functional segments. Remarkable analogies between the peptide-PEG and the corresponding [Tla/Michael]-PEG conjugates sets were indicated by proving similar sensitivity of the payload capacity on the central side chain alternation (e.g., Leu/Leu-analogue → Val/Val-analogue). Moreover, the [Tla/Michael]-PEG closely mimicked the behavior of the peptide-PEG by reaching the highest initial release rates of solubilized *m*-THPC with the Ala/Ala-analogue and showing a rate decrease in the order of Ala, Leu, and Val (analogues) residues. The translation of peptide side-chain sequences into backbones of precision polymers proved to assist the design of functional precision polymer sequences. The approach has been effectively expanded from precision polymers with backbone structure/chemistry that is closely related to peptides, toward peptide-unrelated precision polymer backbones that strongly differ in structure and chemistry. However, property testing will always be required to confirm the function as it can be expected that not only side-chain functionality sequences, but also backbone chemistry, structure, dimensions, and conformational dynamics have a strong contribution to constitute the final function and/or property in the precision polymers.

Experimental Section

Materials, instrumentation, experimental procedures, and analytical data are available in the Supporting Information.

Supporting Information

Supporting Information is available from the Wiley Online Library or from the author.

Acknowledgements

The authors acknowledge M. Senge (Trinity College Dublin) for providing *m*-THPC; Prof. F. Du Prez and S. Martens (Ghent University) for scientific discussions; as well as M. Ballauff and Z. Kochovski (HU, HZB) for CryoTEM. Financial support was granted by the European Research Council under the European Union's 7th Framework Program (FP07–13)/ERC Consolidator grant "Specifically Interacting Polymer-SIP" (ERC 305064) and the European Commission in the Horizon2020 program (EU-ITN EuroSequences Proposal no. 642083).

Conflict of Interest

The authors declare no conflict of interest.

Keywords

drug delivery, functional precision polymers, peptidomimetics, photodynamic therapy, photosensitizer, sequence design

Received: July 9, 2019
Revised: August 9, 2019
Published online: September 4, 2019

[1] T. A. Martinek, F. Fülöp, *Chem. Soc. Rev.* **2012**, *41*, 687.
[2] J. Vagner, H. Qu, V. J. Hruby, *Curr. Opin. Chem. Biol.* **2008**, *12*, 292.
[3] Y. Feng, Y.-Y. Zhang, K. Li, N. Tian, W.-B. Wang, Q.-X. Zhou, X.-S. Wang, *New J. Chem.* **2018**, *42*, 3192.
[4] E. A. Porter, B. Weisblum, S. H. Gellman, *J. Am. Chem. Soc.* **2002**, *124*, 7324.
[5] B. M. deRonde, A. Birke, G. N. Tew, *Chem. - Eur. J.* **2015**, *21*, 3013.
[6] N. Umezawa, M. A. Gelman, M. C. Haigis, R. T. Raines, S. H. Gellman, *J. Am. Chem. Soc.* **2002**, *124*, 368.
[7] K. Gademann, M. Ernst, D. Hoyer, D. Seebach, *Angew. Chem., Int. Ed.* **1999**, *38*, 1223.
[8] N. Tamilarasu, I. Huq, T. M. Rana, *J. Am. Chem. Soc.* **1999**, *121*, 1597.
[9] N. Tamilarasu, I. Huq, T. M. Rana, *Bioorg. Med. Chem. Lett.* **2001**, *11*, 505.
[10] R. Liu, X. Li, K. S. Lam, *Curr. Opin. Chem. Biol.* **2017**, *38*, 117.
[11] S. Mimmi, D. Maisano, I. Quinto, E. Iaccino, *Trends Pharmacol. Sci.* **2019**, *40*, 87.
[12] R. Liu, A. M. Enstrom, K. S. Lam, *Exp. Hematol.* **2003**, *31*, 11.
[13] F. Breitling, A. Nesterov, V. Stadler, T. Felgenhauer, F. R. Bischoff, *Mol. BioSyst.* **2009**, *5*, 224.
[14] K. F. Medzihradszky, R. J. Chalkley, *Mass Spectrom. Rev.* **2015**, *34*, 43.
[15] J. Hentschel, H. G. Börner, *J. Am. Chem. Soc.* **2006**, *128*, 14142.
[16] J. C. Brendel, J. Sanchis, S. Catrouillet, E. Czuba, M. Z. Chen, B. M. Long, C. Nowell, A. Johnston, K. A. Jolliffe, S. Perrier, *Angew. Chem., Int. Ed.* **2018**, *57*, 16678.
[17] R. J. Hafner, L. Tian, J. C. Brauer, T. Schmaltz, A. Sienkiewicz, S. Balog, V. Flauraud, J. Brugger, H. Frauenrath, *ACS Nano* **2018**, *12*, 9116.
[18] J. B. Matson, S. I. Stupp, *Chem. Commun.* **2012**, *48*, 26.
[19] S. Kessel, A. Thomas, H. G. Börner, *Angew. Chem., Int. Ed.* **2007**, *46*, 9023.
[20] S. Große, P. Wilke, H. G. Börner, *Angew. Chem., Int. Ed.* **2016**, *55*, 11266.
[21] T. Schwemmer, J. Baumgartner, D. Faivre, H. G. Börner, *J. Am. Chem. Soc.* **2012**, *134*, 2385.
[22] K. A. Günay, D. Benczédi, A. Herrmann, H.-A. Klok, *Adv. Funct. Mater.* **2017**, *27*, 1603843.
[23] F. Hanßke, O. Bas, C. Vaquette, G. Hochleitner, J. Groll, E. Kemnitz, D. W. Hutmacher, H. G. Börner, *J. Mater. Chem. B* **2017**, *5*, 5037.
[24] J. Horsch, P. Wilke, M. Pretzler, S. Seuss, I. Melnyk, D. Remmler, A. Fery, A. Rompel, H. G. Börner, *Angew. Chem., Int. Ed.* **2018**, *57*, 15728.
[25] E. Maron, J. H. Swisher, J. J. Haven, T. Y. Meyer, T. Junkers, H. G. Börner, *Angew. Chem. Int. Ed.* **2019**, *58*, 10747.
[26] S. Wieczorek, E. Krause, S. Hackbarth, B. Röder, A. K. H. Hirsch, H. G. Börner, *J. Am. Chem. Soc.* **2013**, *135*, 1711.
[27] H. G. Börner, *Prog. Polym. Sci.* **2009**, *34*, 811.
[28] L. Hartmann, H. G. Börner, *Adv. Mater.* **2009**, *21*, 3425.
[29] J.-F. Lutz, M. Ouchi, D. R. Liu, M. Sawamoto, *Science* **2013**, *341*, 1238149.
[30] J.-F. Lutz, *Macromol. Rapid Commun.* **2017**, *38*, 1700582.
[31] O. Altintas, C. Barner-Kowollik, *Macromol. Rapid Commun.* **2016**, *37*, 29.
[32] H. G. Börner, *Macromol. Rapid Commun.* **2011**, *32*, 115.
[33] J.-F. Lutz, J.-M. Lehn, E. W. Meijer, K. Matyjaszewski, *Nat. Rev. Mater.* **2016**, *1*, 16024.
[34] A. Al Ouahabi, L. Charles, J.-F. Lutz, *J. Am. Chem. Soc.* **2015**, *137*, 5629.
[35] M. Ouchi, M. Sawamoto, *Polym. J.* **2018**, *50*, 83.
[36] N. Zydziak, W. Konrad, F. Feist, S. Afonin, S. Weidner, C. Barner-Kowollik, *Nature Commun.* **2016**, *7*, 13672.
[37] J. J. Haven, J. Vandenbergh, R. Kurita, J. Gruber, T. Junkers, *Polym. Chem.* **2015**, *6*, 5752.
[38] S. C. Solleder, D. Zengel, K. S. Wetzel, M. A. R. Meier, *Angew. Chem., Int. Ed.* **2016**, *55*, 1204.
[39] R. N. Zuckermann, J. M. Kerr, S. B. H. Kent, W. H. Moos, *J. Am. Chem. Soc.* **1992**, *114*, 10646.
[40] L. Hartmann, *Macromol. Chem. Phys.* **2011**, *212*, 8.
[41] S. C. Solleder, M. A. R. Meier, *Angew. Chem., Int. Ed.* **2014**, *53*, 711.
[42] S. Martens, A. Landuyt, P. Espeel, B. Devreese, P. Dawyndt, F. Du Prez, *Nat. Commun.* **2018**, *9*, 4451.
[43] P. Espeel, L. L. G. Carrette, K. Bury, S. Capenberghs, J. C. Martins, F. E. Du Prez, A. Madder, *Angew. Chem., Int. Ed.* **2013**, *52*, 13261.
[44] S. Martens, J. van den Begin, A. Madder, F. E. Du Prez, P. Espeel, *J. Am. Chem. Soc.* **2016**, *138*, 14182.
[45] S. Celasun, D. Remmler, T. Schwaar, M. G. Weller, F. Du Prez, H. G. Börner, *Angew. Chem., Int. Ed.* **2019**, *58*, 1960.
[46] S. Wieczorek, D. Remmler, T. Masini, Z. Kochovski, A. K. H. Hirsch, H. G. Börner, *Bioconjugate Chem.* **2017**, *28*, 760.
[47] D. Eckhardt, M. Groenewolt, E. Krause, H. G. Börner, *Chem. Commun.* **2005**, *2005*, 2814.
[48] S. Celasun, F. E. Du Prez, H. G. Börner, *Macromol. Rapid Commun.* **2017**, *38*, 1700688.
[49] R. Gref, Y. Minamitake, M. T. Peracchia, V. Trubetskoy, V. Torchilin, R. Langer, *Science* **1994**, *263*, 1600.
[50] D. Remmler, T. Schwaar, M. Pickhardt, C. Donth, E. Mandelkow, M. G. Weller, H. G. Börner, *J. Controlled Release* **2018**, *285*, 96.
[51] M. Barz, R. Luxenhofer, R. Zentel, M. J. Vicent, *Polym. Chem.* **2011**, *2*, 1900.
[52] H. Ringsdorf, *J. Appl. Polym. Sci.: Polym. Symp.* **1975**, *51*, 135.
[53] M. O. Senge, *Photodiagn. Photodyn. Ther.* **2012**, *9*, 170.
[54] T. H. Foster, B. R. Giesselman, R. Hu, M. E. Kenney, S. Mitra, *Transl. Oncol.* **2010**, *3*, 135.
[55] C. Hopper, A. Kübler, H. Lewis, I. B. Tan, G. Putnam, *Int. J. Cancer* **2004**, *111*, 138.